



# HHS Public Access

Author manuscript

*J Bone Miner Res.* Author manuscript; available in PMC 2017 November 01.

Published in final edited form as:

*J Bone Miner Res.* 2016 November ; 31(11): 2001–2007. doi:10.1002/jbmr.2877.

## Targeting of Mesenchymal Stromal Cells by *Cre*-Recombinase Transgenes Commonly Used to Target Osteoblast Lineage Cells

Jingzhu Zhang and Daniel C Link

Division of Oncology, Department of Medicine, Washington University School of Medicine, St. Louis, MO, USA

### Abstract

The targeting specificity of tissue-specific *Cre*-recombinase transgenes is a key to interpreting phenotypes associated with their use. The *Ocn-Cre* and *Dmp1-Cre* transgenes are widely used to target osteoblasts and osteocytes, respectively. Here, we used high-resolution microscopy of bone sections and flow cytometry to carefully define the targeting specificity of these transgenes. These transgenes were crossed with *Cxcl12<sup>tgfp</sup>* mice to identify Cxcl12-abundant reticular (CAR) cells, which are a perivascular mesenchymal stromal population implicated in hematopoietic stem/progenitor cell maintenance. We show that in addition to osteoblasts, *Ocn-Cre* targets a majority of CAR cells and arteriolar pericytes. Surprisingly, *Dmp1-Cre* also targets a subset of CAR cells, in which expression of osteoblast-lineage genes is enriched. Finally, we introduce a new tissue-specific *Cre*-recombinase, *Tagln-Cre*, which efficiently targets osteoblasts, a majority of CAR cells, and both venous sinusoidal and arteriolar pericytes. These data show that *Ocn-Cre* and *Dmp1-Cre* target broader stromal cell populations than previously appreciated and may aid in the design of future studies. Moreover, these data highlight the heterogeneity of mesenchymal stromal cells in the bone marrow and provide tools to interrogate this heterogeneity.

### Keywords

BONE HISTOMORPHOMETRY; GENETIC ANIMAL MODELS; OSTEOBLASTS; STROMAL/STEM CELLS

### Introduction

The bone marrow microenvironment contains a heterogeneous population of stromal cells that contribute to the regulation of hematopoiesis. Identifying these stromal cells and the signals they generate has important clinical implications for a number of hematopoietic diseases.<sup>(1,2)</sup> Mesenchymal stromal cells implicated in the maintenance of hematopoietic

Address correspondence to: Daniel C Link, MD, Division of Oncology, Department of Medicine, Washington University, 660 South Euclid Avenue, Campus Box 8007, St. Louis, MO 63110, USA. dlink@dom.wustl.edu.

Additional Supporting Information may be found in the online version of this article.

Authors' roles: JZ and DCL conceived and designed the experiments, analyzed the data, and wrote the manuscript. JZ performed the experiments.

### Disclosures

All authors state that they have no conflicts of interest.

stem cells (HSCs) include endothelial cells, osteoblasts, CXCL12-abundant reticular (CAR) cells, mesenchymal stem cells (MSCs), and arteriolar pericytes.<sup>(3–6)</sup> The use of tissue-specific *Cre*-recombinase transgenes to delete genes of interest from defined stromal cell populations is an established and important technique in the field. Rigorously defining the targeting specificity of the *Cre*-recombinase transgenes is a key to the interpretation of such experiments.

Two *Cre*-recombinase transgenes that are commonly used to target osteolineage cells are *Ocn-Cre* and *Dmp1-Cre*. Osteocalcin (*Ocn*, *Bglap*) is a secreted protein implicated in bone and glucose metabolism.<sup>(7)</sup> Cell culture and in situ expression studies show that OCN expression is mostly limited to osteoblasts and osteocytes.<sup>(7,8)</sup> This has led to the widespread use of *Ocn-Cre* transgenes to specifically target osteoblasts and osteocytes.<sup>(9,10)</sup> Dentin matrix acidic phosphoprotein 1 (*Dmp1*) is expressed in odontoblasts, preosteocytes, and osteocytes.<sup>(11,12)</sup> Indeed, a transgene containing an 8-kb regulatory region of *Dmp1* linked to GFP results in osteocyte-specific GFP expression in the bone marrow.<sup>(13)</sup> These data have led to the widespread use of *Dmp1-Cre* transgenes to specifically target osteocytes, although targeting of some osteoblasts also has been observed.<sup>(12,14,15)</sup> Further, a study by Kalajzic and colleagues<sup>(12)</sup> showed that a 10-kb *Dmp1-Cre* transgene targeted both osteoblasts and osteocytes, as well as a small population of undefined cells in the bone marrow.

In the present study, we used high-resolution microscopy of bone sections and flow cytometry to carefully define the targeting specificity of *Ocn-Cre* and *Dmp1-Cre* in the bone marrow. We showed that both the *Ocn-Cre* and *Dmp1-Cre* transgenes target a much broader population of bone marrow stromal cells than previously appreciated. We also characterized for the first time the spectrum of bone marrow stromal cells targeted by a *Tagln-Cre* transgene. We show that *Tagln-Cre* efficiently targets osteoblasts and perivascular stromal cells, but not endothelial cells.

## Materials and Methods

### Mouse strains

*Ai9* (B6.Cg-Gt(ROSA)26Sor<sup>tm9</sup>(CAG-tdTomato)Hze/J)<sup>(16)</sup> mice and *Tagln-Cre* (B6.129S6-*Tagln*<sup>tm2(cre)</sup>Yec/J) mice were obtained from The Jackson Laboratories (Bar Harbor, ME, USA).<sup>(17)</sup> *Ocn-Cre* mice were a gift from Thomas Clemens (Johns Hopkins University, Baltimore, MD, USA).<sup>(18)</sup> *Cxcl12<sup>gfp</sup>* mice were a gift from Takashi Nagasawa (Kyoto University, Kyoto, Japan),<sup>(19)</sup> and *Dmp1-Cre* mice (containing the 9.6-kb murine *Dmp1* promoter) were a gift from Roberto Civitelli (Washington University, St. Louis, MO, USA).<sup>(20)</sup> All mice used in this study were 8 to 10 weeks old. Both male and female mice were used equally in these studies. Genotyping primers are listed in Supporting Table 1. Mice were maintained under specific pathogen free (SPF) conditions, and all experimental procedures were performed according to methods approved by the Animal Studies Committee at Washington University.

## Flow cytometry

Bone marrow cells were harvested from mouse femurs by first uncapping the ends of the bone and then centrifuging at  $3300 \times g$  for 5 min to expel the bone marrow contents. These cells were then digested with 1.67 mg/mL of type II collagenase (Worthington Biochemical, Lakewood, NJ, USA) in phosphate-buffered saline (PBS) for 12 min at  $37^{\circ}\text{C}$ . Of note, the majority of osteoblasts are not recovered using this procedure (Supporting Fig. 1). The following antibodies were used: CD45 (30-F11), CD31 (390), and Ter119 (TER-119). Cells were analyzed on a Gallios flow cytometer (Beckman Coulter, Pasadena, CA, USA), and data analysis was done using FloJo version 10.0.7 software (TreeStar/FlowJo LLC, Ashland, OR, USA).

To sort *Dmp1-Cre*-targeted or *Dmp1-Cre*-non-targeted CAR cells, we first isolated platelet-derived growth factor receptor-beta (PDGFR $\beta$ )-positive stromal cells from the bone marrow of *Dmp1-Cre ROSA26<sup>Ai9/+</sup> Cxcl12<sup>gfp/+</sup>* mice using the AutoMacs Pro Separator system (Miltenyi Biotec, San Diego, CA, USA) and a biotinylated anti-PDGFR $\beta$  antibody (APB5). Cells were incubated with antibodies against Gr-1 (RB6-8C5), PDGFR $\beta$  (APB5), CD45 (30-F11), CD31 (390), and Ter119 (TER-119) and then incubated with brilliant violet 421-conjugated Streptavidin (405225; BioLegend, San Diego, CA, USA). CAR cells were identified as *Cxcl12-GFP<sup>bright</sup> PDGFR $\beta$ <sup>+</sup> Gr1<sup>-</sup> CD45<sup>-</sup> CD31<sup>-</sup> Ter119<sup>-</sup>* cells. *Dmp1-Cre*-targeted CAR cells were tdTomato<sup>high</sup>. Cells were sorted using a MoFlo high-speed flow cytometer (Dako Cytomation, Carpinteria, CA, USA). All antibodies were obtained from eBioscience (San Diego, CA, USA), unless otherwise noted.

## Immunostaining of bone sections

Mouse hindlimbs were fixed in PBS containing 4% paraformaldehyde, pH 7.4, for 24 hours at  $4^{\circ}\text{C}$ . Bones were then decalcified in PBS containing 14% EDTA, pH 7.4, for 7 days at  $4^{\circ}\text{C}$ . Following incubation in PBS containing 30% sucrose for 24 hours at  $4^{\circ}\text{C}$ , bones were embedded in Optimal Cutting Temperature Compound (Sakura Finetek, Torrance, CA, USA). These tissue blocks were cut into 12- $\mu\text{m}$  sections using a Leica Cryo-Jane system (Leica Biosystems, Wetzlar, Germany). For immunostaining, the slides were blocked with 10% donkey serum, diluted in 0.1M Tris-Cl pH 7.5, 150 mM NaCl, and 0.1% Tween 20 (TNT) buffer for 1 hour at room temperature. Following blocking using the Avidin/Biotin Blocking Kit (SP-2001; Vector Laboratories, Burlingame, CA, USA), slides were then incubated in primary antibody overnight at  $4^{\circ}\text{C}$  and, where applicable, they were incubated with secondary antibody for 1 hour at room temperature. The following antibodies were used: rabbit anti-NG2 (AB5320; EMD Millipore, Billerica, MA, USA), rat anti-Sca1 (557403; BD Biosciences, San Jose, CA, USA), goat anti-VECadherin (AF1002; R&D Systems, Minneapolis, MN, USA), mouse anti- $\alpha$ SMA (1A4; Sigma Aldrich, St. Louis, MO, USA); AlexaFluor 488-conjugated donkey anti-rat IgG (Jackson ImmunoResearch, West Grove, PA, USA); DyLight649-conjugated donkey anti-rat IgG (Jackson ImmunoResearch), and biotin-conjugated donkey anti-goat IgG (Jackson ImmunoResearch). In some cases, slides were then incubated with streptavidin-DyLight 649 (Jackson ImmunoResearch) for 1 hour at room temperature. Finally, slides were mounted with ProLong Gold antifade reagent with DAPI (Life Technologies, Inc., Grand Island, NY, USA). Images were acquired with a

LSM 700 microscope (Carl Zeiss Microscopy, Peabody, MA, USA) and processed using Volocity software (PerkinElmer, Waltham, MA, USA).

For hematoxylin and eosin (H&E) staining, bone sections were air dried for 1 hour and then incubated with Hematoxylin Gill #3 (GHS316; Sigma-Aldrich) for 5 min followed by incubation with Eosin (HT110132; Sigma-Aldrich) for 3 min. Sections were then fixed by serial 5-min incubations in 50%, 70%, 95%, and 100% ethanol, followed by a 5-min incubation in xylene. Finally, slides were mounted with Permount mounting medium (Fisher Chemical, Pittsburgh, PA, USA). Images were acquired with a LSM 700 microscope (Carl Zeiss Microscopy).

### RNA expression profiling

RNA was purified from sorted CAR cells using the Qiagen RNeasy Micro Kit (74004; Qiagen, Valencia, CA, USA). Libraries were generated using the NuGen Pico SL kit (NuGEN Technologies, San Carlos, CA, USA) and then hybridized to Affymetrix Mouse Gene 1.0 ST arrays (Affymetrix, Santa Clara, CA, USA). Gene set enrichment was performed using the GSEA software (Broad Institute, Cambridge, MA, USA). Differences in gene expression were determined using Significance Analysis of Microarrays (SAM; Stanford University, Stanford, CA, USA). Expression data has been submitted to Gene Expression Omnibus, record number GSE81399.

### Statistical analyses

Unpaired *t* test was used to evaluate the significance of differences between two groups. All data are presented as mean  $\pm$  SD.

## Results

### *Ocn-Cre* targets osteoblasts, a majority of CAR cells, and arteriolar pericytes

To characterize the targeting specificity of *Ocn-Cre* in postnatal mouse bones, we generated *Ocn-Cre ROSA26<sup>Ai9/+</sup>* mice and *Ocn-Cre ROSA26<sup>Ai9/+</sup> Cxcl12<sup>gfp/+</sup>* mice. The *Cxcl12<sup>gfp/+</sup>* transgene allows for the identification of CXCL12-GFP<sup>bright</sup> (CAR) cells, which are perivascular stromal cells in the bone marrow implicated in HSC maintenance.<sup>(3)</sup> The *ROSA26<sup>Ai9/+</sup>* transgene allows for the identification of *Ocn-Cre*-targeted tdTomato<sup>+</sup> cells. Immunostaining of the bone sections confirmed that the *Ocn-Cre* transgene efficiently targets osteoblasts (Fig. 1A, B; Supporting Fig. 2).<sup>(18)</sup> Surprisingly, we also observed that *Ocn-Cre* targets a substantial fraction of CXCL12-GFP<sup>bright</sup> cells (Fig. 1A, C). Of note, as expected, no tdTomato<sup>+</sup> CAR cells were detected in control (*Cxcl12<sup>gfp/+</sup>*) mice (Supporting Fig. 3). Flow cytometry showed that *Ocn-Cre* targets 72.2%  $\pm$  4.0% (*n* = 3 mice) of CXCL12-GFP<sup>bright</sup> cells (Fig. 1D). To assess targeting of arteriolar pericytes, we stained bone sections from wild-type mice with antibodies against alpha-smooth muscle actin ( $\alpha$ SMA) and NG2 (Fig. 2A, B). In these assays, arteriolar endothelial cells were identified by Sca1,<sup>(6)</sup> which is also expressed on hematopoietic stem/progenitor cells but not on CAR cells.<sup>(4)</sup> Whereas  $\alpha$ SMA staining was limited to a subset of arteriolar pericytes, NG2 staining was observed in all arteriolar pericytes (Fig. 2A, B). Accordingly, all  $\alpha$ SMA-positive arteriolar pericytes co-expressed NG2, while only 56.9%  $\pm$  11.1% (*n* = 3 mice) of

NG2-positive arteriolar pericytes co-expressed  $\alpha$ SMA. Immunostaining of bone sections from *Ocn-Cre ROSA26<sup>Ai9/+</sup>* mice showed that *Ocn-Cre* targets  $72.2\% \pm 13.3\%$  ( $n = 3$  mice) of NG2-positive arteriolar pericytes (Fig. 2C). Thus, in addition to osteoblasts, *Ocn-Cre* targets the majority of CAR cells and arteriolar pericytes in mice.

### ***Dmp1-Cre* targets osteoblasts and a subset of CAR cells**

To characterize the targeting specificity of *Dmp1-Cre* in postnatal mouse bones, we generated *Dmp1-Cre ROSA26<sup>Ai9/+</sup>* mice and *Dmp1-Cre ROSA26<sup>Ai9/+</sup> Cxcl12<sup>gfp/+</sup>* mice. As reported,<sup>(15,20)</sup> the *Dmp1-Cre* transgene efficiently targets all osteoblasts (Fig. 3A, B; Supporting Fig. 4). Surprisingly, *Dmp1-Cre* also targets a subset of CAR cells (Fig. 3A, C). Interestingly, *Dmp1-Cre*-targeted CAR cells were not enriched near the endosteum or osteoblasts, but were distributed throughout the bone marrow (Supporting Fig. 5A, B). By flow cytometry  $29.2\% \pm 1.7\%$  ( $n = 3$  mice) of CAR cells are targeted by *Dmp1-Cre* (Fig. 3D). In contrast to *Ocn-Cre*, NG2<sup>+</sup> arteriolar pericytes were rarely targeted by *Dmp1-Cre* (Fig. 3E). Thus, *Dmp1-Cre* targets all osteoblasts and a subset of CAR cells but few arteriolar pericytes.

To characterize the *Dmp1-Cre*-targeted subset of CAR cells, we sorted tdTomato<sup>+</sup> (*Dmp1-Cre*-targeted) and tdTomato<sup>-</sup> CAR cells (*Dmp1-Cre*-non-targeted) and performed RNA expression profiling. Gene set enrichment analysis showed that *Dmp1-Cre*-targeted CAR cells were highly enriched for a previously identified group of genes involved in osteoblast maturation or bone development (Supporting Fig. 6A). Indeed, expression of genes associated with mature osteoblasts such as *Bglap2* (*Ocn*) and *Postn* (periostin) are increased nearly fourfold compared to non-targeted CAR cells (Fig. 3F). In contrast, expression of early osteoblast lineage genes, including *Sp7* (osterix) and *Runx2* were normal or only minimally elevated (Fig. 3F). Expression of key HSC maintenance genes (*Cxcl12*, *Kitl*, and *Angpt1*) or key B lymphoid factor genes (*Igf1*, *Flt3l*, or *BAFF*) was similar in *Dmp1-Cre*-targeted and *Dmp1-Cre*-non-targeted CAR cells (Supporting Fig. 6B, C). However, expression of interleukin-7 (IL-7), which is required for pro-B cell maintenance, was significantly reduced in *Dmp1-Cre*-targeted CAR cells.

### ***Tagln-Cre* targets osteoblasts, a majority of CAR cells, and both arteriolar and venous sinusoidal pericytes**

Arteriolar pericytes have been implicated in HSC maintenance and can be readily identified in the bone marrow as Nestin-GFP<sup>bright</sup> or NG2<sup>+</sup> periarteriolar cells.<sup>(6)</sup> However, a recent study reported that a substantial number of functional HSCs localize to venous sinusoids in the central bone marrow.<sup>(21)</sup> In an effort to better visualize and isolate sinusoidal pericytes, we tested targeting by the *Tagln-Cre* transgene. *Tagln* encodes for transgelin (SM22a) and is expressed in smooth muscle cells and cardiomyocytes.<sup>(22–24)</sup> *Tagln* is also expressed in osteoblasts.<sup>(25)</sup> Accordingly, *Tagln-Cre* targets all osteoblasts (Fig. 4A, B; Supporting Fig. 7). Analyzing *Tagln-Cre ROSA26<sup>Ai9/+</sup> Cxcl12<sup>gfp/+</sup>* mice, we observed that *Tagln-Cre* and CXCL12-GFP mark overlapping, but distinct, bone marrow stromal cell populations (Fig. 4B, C). Whereas *Tagln-Cre* targets the great majority of CXCL12-GFP<sup>+</sup> CAR cells that line venous sinusoids which are marked by vascular endothelial cadherin (VE-cadherin),<sup>(6,26)</sup> it does not efficiently target those CXCL12-GFP<sup>+</sup> CAR cells that are not in direct contact with

sinusoids (Fig. 4D, yellow arrows). Conversely, *Tagln-Cre* targets a population of perisinusoidal cells that are CXCL12-GFP dim/negative (Fig. 4D, red arrows), presumably representing non-CAR venous pericytes. Moreover, *Tagln-Cre*, but not CXCL12-GFP, marks periarteriolar pericytes (Fig. 4E). Indeed, *Tagln-Cre* targeted nearly all NG2<sup>+</sup> arteriolar pericytes (Fig. 4E, F). Flow cytometry showed that *Tagln-Cre* targets 74.9% ± 5.2% (*n* = 3 mice) of CAR cells (Fig. 4G). Conversely, 16.6% ± 2.3% (*n* = 3 mice) of *Tagln-Cre*-targeted stromal cells were CXCL12-GFP dim/negative. Collectively, these data show that *Tagln-Cre* efficiently targets all osteoblasts, a majority of CAR cells, and both venous and arteriolar pericytes.

## Discussion

*Ocn-Cre* has been widely used to target osteoblasts in past studies.<sup>(7,9,10)</sup> Our data show that *Ocn-Cre* targets not only osteoblasts, but also more than 70% of CAR cells and arteriolar pericytes. CAR cells are mesenchymal progenitors that have adipogenic and osteogenic capacity in vitro.<sup>(27)</sup> However, only a small subset of CAR cells contributes to osteoblast development in vivo.<sup>(3)</sup> Whether the *Ocn-Cre*-targeted subset of CAR cells is fated to osteoblast differentiation is unclear. Of note, we did not observe preferential localization of *Ocn-Cre*-targeted CAR cells to the endosteal region. CAR cells constitutively produce high levels of multiple cytokines and chemokines that regulate hematopoiesis, including CXCL12 and stem cell factor.<sup>(27)</sup> Indeed, CAR cells have been implicated in the maintenance of HSCs and B lymphoid progenitors.<sup>(28,29)</sup> Thus, phenotypes reported using *Ocn-Cre* need to be interpreted in light of our data showing targeting of CAR cells and arteriolar pericytes, in addition to osteoblasts.

*Dmp1-Cre* has been widely used to target osteocytes.<sup>(12,14,30)</sup> Several *Dmp1-Cre* transgenes have been described. In this study, we show that the 10-kb *Dmp1-Cre* transgene not only efficiently targets osteoblasts, but also targets a subset of CAR cells. The results are consistent with a prior study by Kalajzic and colleagues<sup>(12)</sup> showing that the 10-kb *Dmp1-Cre* transgene targets a small population of undefined cells in the bone marrow, in addition to osteoblasts and osteocytes. Of note, the same group also reported that an 8-kb *Dmp1-Cre* transgene, which is thought to be more osteocyte-restricted, targets, at least a subset of, osteoblasts.<sup>(12)</sup> Whether the 8-kb *Dmp1-Cre* transgene targets a subset of CAR cells will require further study. Our data show that the 10-kb *Dmp1-Cre* transgene targets approximately 30% of CAR cells. Expression profiling of this subset of CAR cells shows higher expression of genes associated with mature osteoblasts, suggesting that *Dmp1-Cre*-targeted CAR cells may be enriched for osteoprogenitors. Functional studies are needed to confirm this possibility.

We report for the first time the spectrum of bone marrow stromal cells that are targeted by a *Tagln-Cre* transgene. Prior studies in non-bone tissues had shown transgelin expression in cardiomyocytes and vascular smooth muscle cells.<sup>(22–24)</sup> Consistent with its expression in osteoblasts,<sup>(25)</sup> *Tagln-Cre* efficiently targets osteoblasts. Interestingly, *Tagln-Cre* appears to target a majority of CAR cells. Specifically, it targets those CAR cells that are closely associated with venous sinusoids (ie, venous sinusoidal pericytes). Conversely, *Tagln-Cre* does not efficiently target CAR cells that are more distant from sinusoids. Finally, *Tagln-Cre*

efficiently targets arteriolar pericytes, which, despite evidence for high CXCL12 expression,<sup>(6)</sup> do not express high-level GFP in *Cxcl12<sup>gfp</sup>* mice. Thus, the *Tagln-Cre* represents an important new tool for investigators to efficiently target both venous sinusoidal and arteriolar pericytes in the bone marrow.

This study highlights the complexity and heterogeneity of mesenchymal stromal cells in the bone marrow. Nestin-GFP<sup>+</sup>, LepR<sup>+</sup>, and CAR cells represent overlapping but not identical populations of perivascular mesenchymal stromal cells.<sup>(3,5,29,31)</sup> Bulk cell analysis of each of these populations shows high-level expression of genes that regulate hematopoiesis, including factors that regulate HSCs (eg, kit ligand) and B lymphopoiesis (eg, IL-7).<sup>(3,28,29,31)</sup> Our study suggests that there is considerable heterogeneity within the CAR cell population. For example, the *Dmp1-Cre*-targeted subset of CAR cells, in addition to being enriched for osteoblast genes, expresses a lower level of IL-7. IL-7-producing stromal cells in the bone marrow are required for the maintenance of Pro-B cells,<sup>(28)</sup> suggesting that *Dmp1-Cre*-targeted CAR cells likely do not contribute to this specific stage of B cell development.

In summary, we have rigorously defined the targeting specificities in the bone marrow for the three *Cre*-recombinase transgenes. *Ocn-Cre* and *Dmp1-Cre* target broader stromal cell populations than previously appreciated, and this data should be incorporated into the design of future studies. These data further highlight the heterogeneity of mesenchymal stromal cells in the bone marrow, and suggest that the *Cre*-recombinase transgenes used in this study could be used to interrogate this heterogeneity.

## Supplementary Material

Refer to Web version on PubMed Central for supplementary material.

## Acknowledgments

This work was supported by RO1 HL60772 (to DCL) and P50 CA171963 (to DCL). We thank Amy Schmidt for technical assistance and Jackie Tucker-Davis for animal care.

## References

1. Morrison SJ, Scadden DT. The bone marrow niche for haematopoietic stem cells. *Nature*. 2014; 505(7483):327–34. [PubMed: 24429631]
2. Ding L, Morrison SJ. Haematopoietic stem cells and early lymphoid progenitors occupy distinct bone marrow niches. *Nature*. 2013; 495(7440):231–5. [PubMed: 23434755]
3. Calvi LM, Link DC. Cellular complexity of the bone marrow hematopoietic stem cell niche. *Calcif Tissue Int*. 2014; 94(1):112–24. [PubMed: 24101231]
4. Greenbaum A, Hsu YM, Day RB, et al. CXCL12 in early mesenchymal progenitors is required for haematopoietic stem-cell maintenance. *Nature*. 2013; 495(7440):227–30. [PubMed: 23434756]
5. Ding L, Saunders TL, Enikolopov G, Morrison SJ. Endothelial and perivascular cells maintain haematopoietic stem cells. *Nature*. 2012; 481(7382):457–62. [PubMed: 22281595]
6. Kunisaki Y, Bruns I, Scheiermann C, et al. Arteriolar niches maintain haematopoietic stem cell quiescence. *Nature*. 2013; 502(7473):637–43. [PubMed: 24107994]
7. Brennan-Speranza TC, Conigrave AD. Osteocalcin: an osteoblast-derived polypeptide hormone that modulates whole body energy metabolism. *Calcif Tissue Int*. 2015; 96(1):1–10. [PubMed: 25416346]

8. Lee NK, Sowa H, Hinoi E, et al. Endocrine regulation of energy metabolism by the skeleton. *Cell*. 2007; 130(3):456–69. [PubMed: 17693256]
9. Burgers TA, Hoffmann MF, Collins CJ, et al. Mice lacking pten in osteoblasts have improved intramembranous and late endochondral fracture healing. *PLoS One*. 2013; 8(5):e63857. [PubMed: 23675511]
10. Zhong Z, Zylstra-Diegel CR, Schumacher CA, et al. Wntless functions in mature osteoblasts to regulate bone mass. *Proc Natl Acad Sci U S A*. 2012; 109(33):E2197–204. [PubMed: 22745162]
11. Qin C, D'Souza R, Feng JQ. Dentin matrix protein 1 (DMP1): new and important roles for biomineralization and phosphate homeostasis. *J Dent Res*. 2007; 86(12):1134–41. [PubMed: 18037646]
12. Kalajzic I, Matthews BG, Torreggiani E, Harris MA, Divieti Pajevic P, Harris SE. In vitro and in vivo approaches to study osteocyte biology. *Bone*. 2013; 54(2):296–306. [PubMed: 23072918]
13. Kalajzic I, Braut A, Guo D, et al. Dentin matrix protein 1 expression during osteoblastic differentiation, generation of an osteocyte GFP-transgene. *Bone*. 2004; 35(1):74–82. [PubMed: 15207743]
14. Xiao Z, Huang J, Cao L, Liang Y, Han X, Quarles LD. Osteocyte-specific deletion of Fgfr1 suppresses FGF23. *PLoS One*. 2014; 9(8):e104154. [PubMed: 25089825]
15. Xiong J, Onal M, Jilka RL, Weinstein RS, Manolagas SC, O'Brien CA. Matrix-embedded cells control osteoclast formation. *Nat Med*. 2011; 17(10):1235–41. [PubMed: 21909103]
16. Madisen L, Zwingman TA, Sunkin SM, et al. A robust and high-throughput Cre reporting and characterization system for the whole mouse brain. *Nat Neurosci*. 2010; 13(1):133–40. [PubMed: 20023653]
17. Zhang J, Zhong W, Cui T, et al. Generation of an adult smooth muscle cell-targeted Cre recombinase mouse model. *Arterioscler Thromb Vasc Biol*. 2006; 26(3):e23–4. [PubMed: 16484601]
18. Zhang M, Xuan S, Bouxsein ML, et al. Osteoblast-specific knockout of the insulin-like growth factor (IGF) receptor gene reveals an essential role of IGF signaling in bone matrix mineralization. *J Biol Chem*. 2002; 277(46):44005–12. [PubMed: 12215457]
19. Ara T, Itoi M, Kawabata K, et al. A role of CXC chemokine ligand 12/stromal cell-derived factor-1/pre-B cell growth stimulating factor and its receptor CXCR4 in fetal and adult T cell development in vivo. *J Immunol*. 2003; 170(9):4649–55. [PubMed: 12707343]
20. Lu Y, Xie Y, Zhang S, Dusevich V, Bonewald LF, Feng JQ. DMP1-targeted Cre expression in odontoblasts and osteocytes. *J Dent Res*. 2007; 86(4):320–5. [PubMed: 17384025]
21. Acar M, Kocherlakota KS, Murphy MM, et al. Deep imaging of bone marrow shows non-dividing stem cells are mainly perisinusoidal. *Nature*. 2015; 526(7571):126–30. [PubMed: 26416744]
22. Umans L, Cox L, Tjwa M, et al. Inactivation of Smad5 in endothelial cells and smooth muscle cells demonstrates that Smad5 is required for cardiac homeostasis. *Am J Pathol*. 2007; 170(5):1460–72. [PubMed: 17456754]
23. Assinder SJ, Stanton JA, Prasad PD. Transgelin: an actin-binding protein and tumour suppressor. *Intl J Biochem Cell Biol*. 2009; 41(3):482–6.
24. El-Bizri N, Guignabert C, Wang L, et al. SM22alpha-targeted deletion of bone morphogenetic protein receptor 1A in mice impairs cardiac and vascular development, and influences organogenesis. *Development*. 2008; 135(17):2981–91. [PubMed: 18667463]
25. Eash KJ, Greenbaum AM, Gopalan PK, Link DC. CXCR2 and CXCR4 antagonistically regulate neutrophil trafficking from murine bone marrow. *J Clin Invest*. 2010; 120(7):2423–31. [PubMed: 20516641]
26. Inra CN, Zhou BO, Acar M, et al. A perisinusoidal niche for extramedullary haematopoiesis in the spleen. *Nature*. 2015; 527(7579):466–71. [PubMed: 26570997]
27. Omatsu Y, Sugiyama T, Kohara H, et al. The essential functions of adipo-osteogenic progenitors as the hematopoietic stem and progenitor cell niche. *Immunity*. 2010; 33(3):387–99. [PubMed: 20850355]
28. Tokoyoda K, Egawa T, Sugiyama T, Choi BI, Nagasawa T. Cellular niches controlling B lymphocyte behavior within bone marrow during development. *Immunity*. 2004; 20(6):707–18. [PubMed: 15189736]



29. Sugiyama T, Kohara H, Noda M, Nagasawa T. Maintenance of the hematopoietic stem cell pool by CXCL12-CXCR4 chemokine signaling in bone marrow stromal cell niches. *Immunity*. 2006; 25(6):977–88. [PubMed: 17174120]
30. Komori T. Mouse models for the evaluation of osteocyte functions. *J Bone Metab*. 2014; 21(1):55–60. [PubMed: 24707467]
31. Mendez-Ferrer S, Michurina TV, Ferraro F, et al. Mesenchymal and haematopoietic stem cells form a unique bone marrow niche. *Nature*. 2010; 466(7308):829–34. [PubMed: 20703299]

Author Manuscript

Author Manuscript

Author Manuscript

Author Manuscript

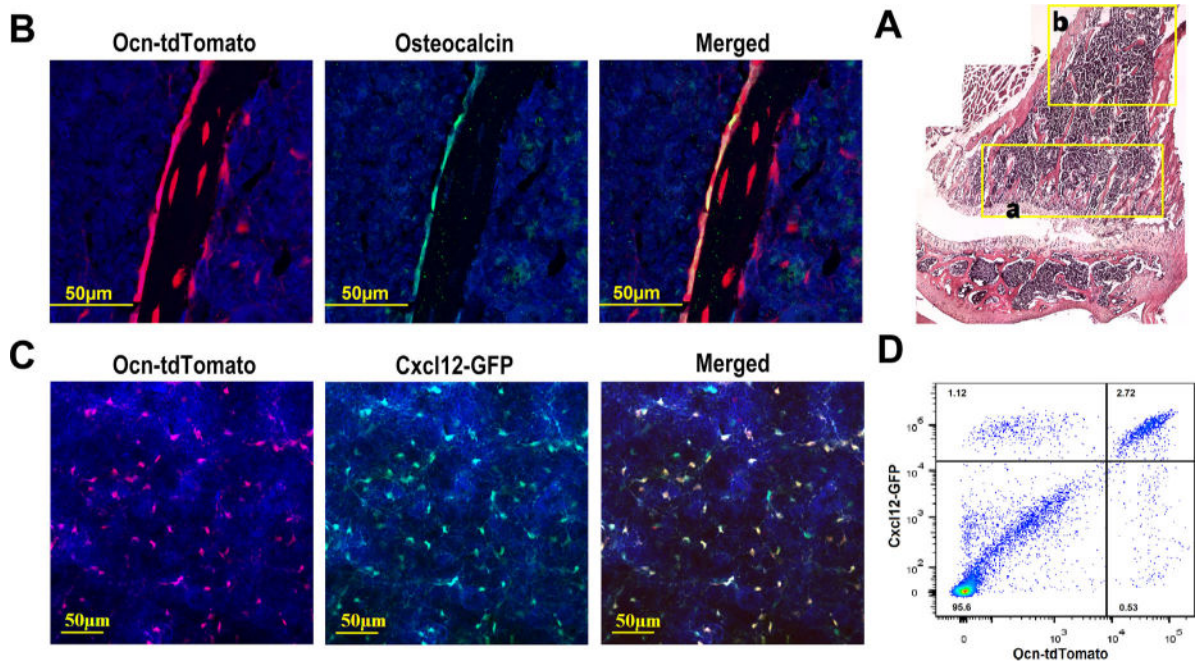


**Fig. 1.**

*Ocn-Cre* targets osteoblasts and a majority of CAR cells. (A) Composite image of H&E stained sections from the femur of an *Ocn-Cre ROSA26<sup>Ai9/+</sup>* mouse. (B) Representative photomicrographs of the metaphyseal region (region “a” in A) of a femur section stained for osteocalcin (green) to mark osteoblasts and DAPI (blue) to highlight nuclei; cells that had undergone *Cre*-mediated recombination express tdTomato (red). (C) Representative photomicrographs taken from the diaphyseal region (similar to region “b” in A) of a femur section from an *Ocn-Cre ROSA26<sup>Ai9/+</sup> Cxcl12<sup>gfp/+</sup>* mouse. Cells that express CXCL12 also express GFP (green). Counterstaining with DAPI highlights nuclei (blue). (D) Representative dot plots showing GFP and tdTomato expression in lineage (CD45, CD31, and Ter119) negative stromal cells harvested from *Ocn-Cre ROSA26<sup>Ai9/+</sup> Cxcl12<sup>gfp/+</sup>* mice. Original magnification,  $\times 200$  except for A, which is  $\times 100$ .

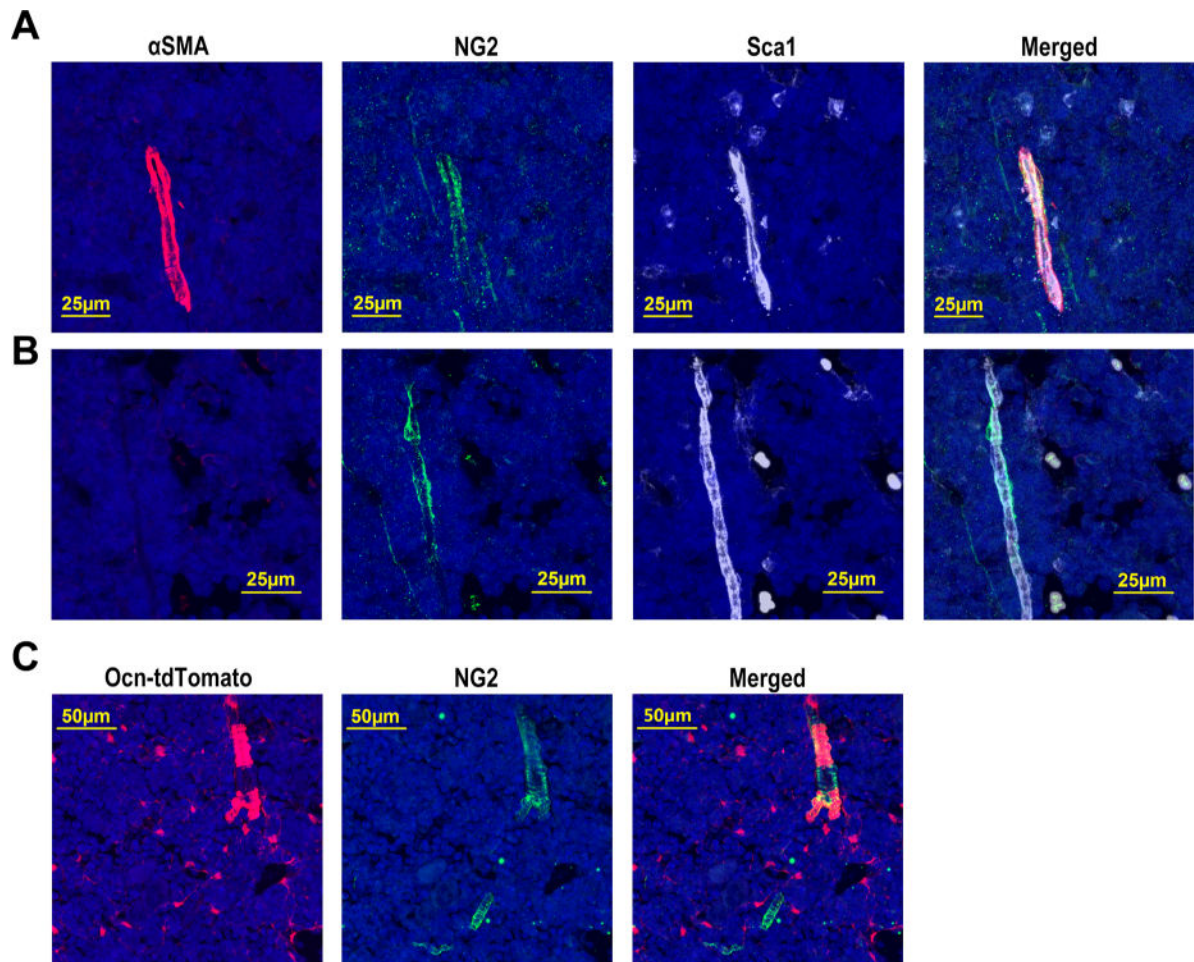


**Fig. 2.**

*Ocn-Cre* targets the majority of arteriolar pericytes. Representative photomicrographs of the diaphyseal region (similar to region “b” in Fig. 1A) of a femur section from a wild-type mouse stained for  $\alpha$ SMA (red), NG2 (green), Sca1 (white), and DAPI (blue). (A) Images showing  $\alpha$ SMA<sup>+</sup> NG2<sup>+</sup> arteriolar pericytes around Sca1<sup>+</sup> arteriolar endothelial cells. (B) Images showing Asma<sup>-</sup> NG2<sup>+</sup> arteriolar pericytes around Sca1<sup>+</sup> arteriolar endothelial cells. (C) Representative photomicrographs of the diaphyseal region of a femur section from an *Ocn-Cre ROSA26<sup>Ai9/+</sup>* mouse stained for NG2 (green) and DAPI (blue). TdTomato (red) represents cells targeted by *Ocn-Cre*. Original magnification,  $\times 200$ .

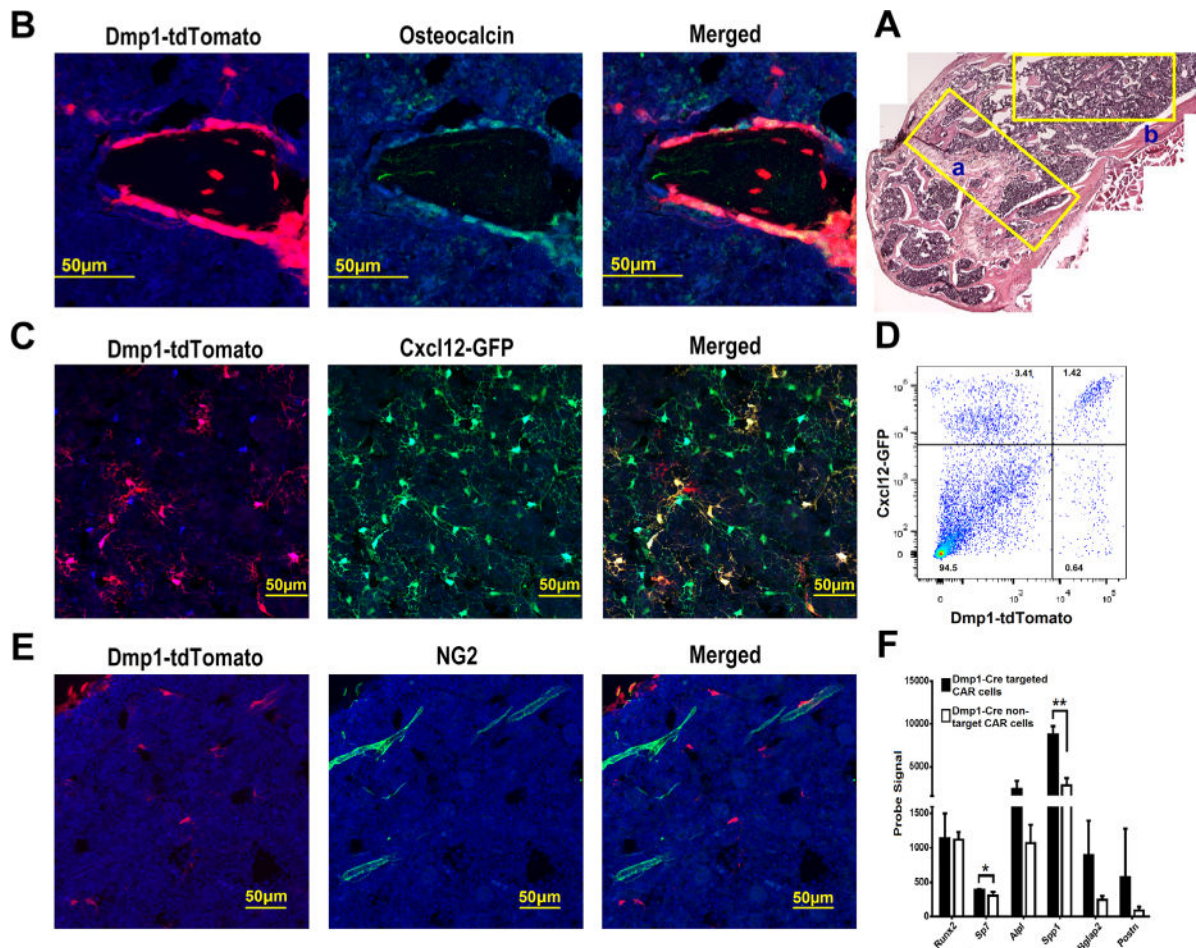


**Fig. 3.** *Dmp1-Cre* targets all the osteoblasts and a subset of CAR cells but no arteriolar pericytes. (A) Composite image of H&E-stained sections from the femur of a *Dmp1-Cre ROSA26<sup>Ai9/+</sup>* mouse. (B) Representative photomicrographs of the metaphyseal region (region “a” in A) of a femur section that was stained for osteocalcin (green) and DAPI (blue). *Dmp1-Cre* targeted cells express tdTomato (red). (C) Representative photomicrographs taken from the diaphyseal region (similar to region “b” in A) of a femur section from a *Dmp1-Cre ROSA26<sup>Ai9/+</sup> Cxcl12<sup>gfp/+</sup>* mouse; cells that express CXCL12 also express GFP (green). (D) Representative dot plot showing GFP and tdTomato expression in lineage (CD45, CD31, and Ter119) negative stromal cells harvested from *Dmp1-Cre ROSA26<sup>Ai9/+</sup> Cxcl12<sup>gfp/+</sup>* mice. (E) Representative photomicrographs taken from the diaphyseal region of a femur section from a *Dmp1-Cre ROSA26<sup>Ai9/+</sup> Cxcl12<sup>gfp/+</sup>* mouse stained for NG2 (green) and DAPI (blue). (F) RNA expression profiling of sorted *Dmp1-Cre* targeted (tdTomato<sup>+</sup>) or non-targeted (tdTomato<sup>-</sup>) CAR cells was performed. Shown are probe signals for the indicated genes ( $n = 3$  mice). All data represent the mean  $\pm$  SD. \* $p < 0.05$ ; \*\* $p < 0.01$  (unpaired  $t$  test). Original magnification,  $\times 200$  except for A, which is  $\times 100$ .

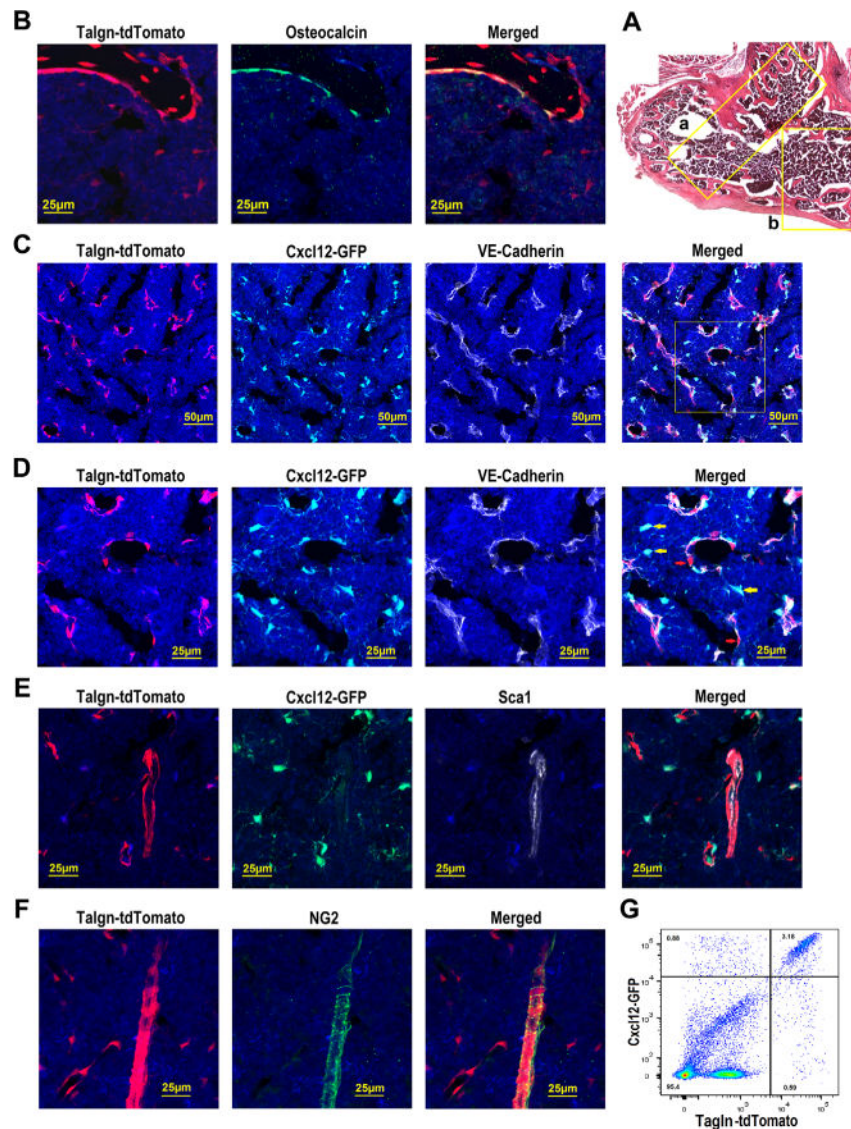


**Fig. 4.** *Tagln-Cre* targets osteoblasts, a majority of CAR cells, and both venous sinusoidal and arteriolar pericytes. (A) Composite image of H&E-stained sections from the femur of a *Tagln-Cre ROSA26<sup>Ai9/+</sup>* mouse. (B) Representative photomicrographs of the metaphyseal region (region “a” in A) of a femur section that was stained for osteocalcin (green) and DAPI (blue). (C) Representative photomicrographs taken from the diaphyseal region (similar to region “b” in A) of a femur section from a *Tagln-Cre ROSA26<sup>Ai9/+</sup> Cxcl12<sup>gfp/+</sup>* mouse stained for VE-cadherin (white) to mark all endothelial cells; cells that express CXCL12 also express GFP (green). (D) Enlarged images of the boxed region in C. (E) Representative photomicrographs taken from the diaphyseal region of a femur section from a *Tagln-Cre ROSA26<sup>Ai9/+</sup> Cxcl12<sup>gfp/+</sup>* mouse stained for Sca1 (white) to mark arteriolar endothelial cells. (F) Representative photomicrographs taken from the diaphyseal region of a femur section from *Tagln-Cre ROSA26<sup>Ai9/+</sup>* mouse stained for NG2 (green) to mark arteriolar pericytes. (G) Representative dot plot of lineage (CD45, CD31, and Ter119) negative

stromal cells from a *Tagln-Cre ROSA26<sup>Ai9/+</sup> Cxcl12<sup>gfp/+</sup>* mouse showing GFP and tdTomato expression. Original magnification,  $\times 200$  except for *A*, which is  $\times 100$ .

Author Manuscript

Author Manuscript

Author Manuscript

Author Manuscript